JOURNAL OF NEUROPHYSIOLOGY
Vol. 71, No. 2, February 1994. *Printed in U.S.A.*

Modeling Three-Dimensional Velocity-to-Position Transformation in Oculomotor Control

CHARLES SCHNABOLK AND THEODORE RAPHAN
Institute of Neural and Intelligent Systems, Department of Computer and Information Science, Brooklyn College of The City University of New York, Brooklyn, New York 11210

SUMMARY AND CONCLUSIONS

1. A considerable amount of attention has been devoted to understanding the velocity-position transformation that takes place in the control of eye movements in three dimensions. Much of the work has focused on the idea that rotations in three dimensions do not commute and that a "multiplicative quaternion model" of velocity-position integration is necessary to explain eye movements in three dimensions. Our study has indicated that this approach is not consistent with the physiology of the types of signals necessary to rotate the eyes.

2. We developed a three-dimensional dynamical system model for movement of the eye within its surrounding orbital tissue. The main point of the model is that the eye muscles generate torque to rotate the eye. When the eye reaches an orientation such that the restoring torque of the orbital tissue counterbalances the torque applied by the muscles, a unique equilibrium point is reached. The trajectory of the eye to reach equilibrium may follow any path, depending on the starting eye orientation and eye velocity. However, according to Euler's theorem, the equilibrium reached is equivalent to a rotation about a fixed axis through some angle from a primary orientation. This represents the shortest path that the eye could take from the primary orientation in reaching equilibrium. Consequently, it is also the shortest path for returning the eye to the primary orientation. Thus the restoring torque developed by the tissue surrounding the eye was approximated as proportional to the product of this angle and a unit vector along this axis. The relationship between orientation and restoring torque gives a unique torque-orientation relationship.

3. Once the appropriate torque-orientation relationship for eye rotation is established the velocity-position integrator can be modeled as a dynamical system that is a direct extension of the one-dimensional velocity-position integrator. The linear combination of the integrator state and a direct pathway signal is converted to a torque signal that activates the muscles to rotate the eyes. Therefore the output of the integrator is related to a torque signal that positions the eyes. It is not an eye orientation signal. The applied torque signal drives the eye to an equilibrium orientation such that the restoring torque equals the applied torque but in the opposite direction. The eye orientation reached at equilibrium is determined by the unique torque-orientation relation. Because torque signals are vectors, they commute. Thus our model indicates that the signals in the CNS can be treated as vectors and that the nonvector orientation properties of the eye globe are inherent in the dynamical system associated with the globe and its underlying tissue.

4. Listing's law is explained very simply by our model as being a property of the vector nature of the signals in the CNS driving the eyes, and its implementation is not localized to any specific locality within the CNS. If the neural vector signal driving the eye is confined to Listing's plane, i.e., the pitch-yaw plane in our model, then eye orientation will obey Listing's law.

5. We performed simulations to show that Listing's law is obeyed by our model for both saccades and smooth pursuit eye movements in the steady state. The simulations also showed that there is commutativity in terms of steady-state eye orientation. We performed simulations that compared the model output with data of others. Deviations from Listing's law were consistent with the physiological findings.

INTRODUCTION

Recordings from abducens motoneurons during sinusoidal vestibular nystagmus suggested that to drive the eyes there must be a central integrator that converts the velocity command signal coming from the eighth nerve into a position signal that projects to the motoneurons (Skavenski and Robinson 1973). The "velocity-to-position integrator," as it has come to be known, functions to transmit information to hold the eyes in a given position in the orbit. It is utilized during slow eye movements as well as during saccades and quick phases of nystagmus (Cohen and Komatsuzaki 1972; Raphan and Cohen 1978; Robinson 1974). There is considerable evidence that the velocity-to-position integrator has dynamics, i.e., a time constant. The time constant appears to be >20–25 s in humans (Becker and Klein 1973) and cats (Robinson 1974) and is capable of holding the eyes in eccentric positions of gaze for long periods of time even in darkness. The dynamics are under parametric control of the cerebellum (Robinson 1974).

Recent attempts to model the velocity-to-position integrator in three dimensions have focused on the three-dimensional rotation operations that relate the orientation of the eye in the head to the eye velocity command (Henn et al. 1992; Hepp 1990; Hepp and Henn 1987; Hepp et al. 1988; Tweed and Vilis 1987, 1988). Tweed and Vilis (1987) argued that because of the noncommutative aspects of eye rotations the velocity command could not just be integrated to generate the position command to the eyes. They used quaternions to represent the rotations and developed a "multiplicative model" whose output was a quaternion representing eye position and having eye velocity as its input. This model treats the orientation of the eye as the output of the velocity-position integrator. It neglects the fact that the CNS activates the muscles that generate the torque to rotate the eye (Collins 1971; Collins et al. 1969; Cook and Stark 1967; Levin and Wyman 1927; Robinson 1964; Robinson et al. 1969). It is the applied torque developed in the muscles, the inertia of the eye, the viscosity of the medium in which it rotates, and the restoring torque that acts to return the globe to a mechanical neutral point

close to the primary position (Robinson 1975b) that determine the position of the eyes as a function of time. Therefore the model developed by Tweed and Vilis (1987) has a nonphysiologic character that does not effectively deal with the dynamics of eye rotation in three dimensions and does not accurately model the velocity-position integrator.

The purpose of our study is to consider the velocity-position integrator as a dynamical system whose output is a signal converted to torque that positions the eyes in relation to the passive restoring torque developed by the orbital tissue. The aim is to show that if the system is viewed in this way the "velocity signal" generated in the CNS to move the eyes can be integrated via a three-dimensional velocity-position integrator. The linear combination of the integrator state and a direct pathway signal activates the muscles to rotate the eyes (Robinson 1964, 1965).

Conceptual development of the model

Early work describing the properties of the eye and its surrounding tissue (plant) showed that in one dimension the plant dynamics could be represented by an overdamped second-order model with a dominant time constant of 0.15 s in humans (Collins 1971; Robinson 1964, 1965). Quick release mechanical experiments in the monkey (Keller and Robinson 1971) gave ~0.09 s. The mean dominant time constant as obtained from a population of motoneurons in monkey was 0.20 s (Robinson 1970). It is not known whether these differences are species related or differences in experimental procedure (Robinson 1973). At any rate, the system in both species is overdamped and a pulse-step of activity is necessary to execute a saccade and hold the eyes in a given position (Robinson 1964, 1973). During slow eye movements, such as pursuit and compensatory slow phases of nystagmus, a step-ramp of torque is needed to drive the eyes (Robinson 1965). Both the pulse-step and the step-ramp could be achieved by a "neural integration" of a velocity command that is superposed directly with the velocity command (Robinson 1975a, 1981) to drive the motoneurons.

The conceptual model of the eye movement positioning mechanism in three dimensions follows this organizational principle and is shown in Fig. 1. The neural input in the model comes from a slow phase velocity command associated with pursuit and head rotation or a saccadic command from the pulse-generating network in the paramedian pontine reticular formation (PPRF) (Cohen and Henn 1972a,b; Cohen and Komatsuzaki 1972; Henn and Cohen 1976; Hepp et al. 1989; Keller 1974) (Fig. 1). The neural input drives the velocity-position integrator dynamical system as well as the direct premotor-to-motoneuron coupling matrix, D. The velocity-position integrator receives input from both saccadic and slow phase modalities. The sum of the output of the velocity-position integrator dynamical system ($\mathbf{x}_p$) and the direct premotor-to-motoneuron coupling drives the motoneurons. The motoneuron signal generates the torque in the muscles to orient the eye, i.e., plant. (Note: boldface characters in text represent vectors.)

When the eye is fixated in a given position an equilibrium is reached between the restoring torque developed because of eye rotation from the primary position and the applied torque from the integrator signal. Thus the state of the integrator is a "position" command that approximates

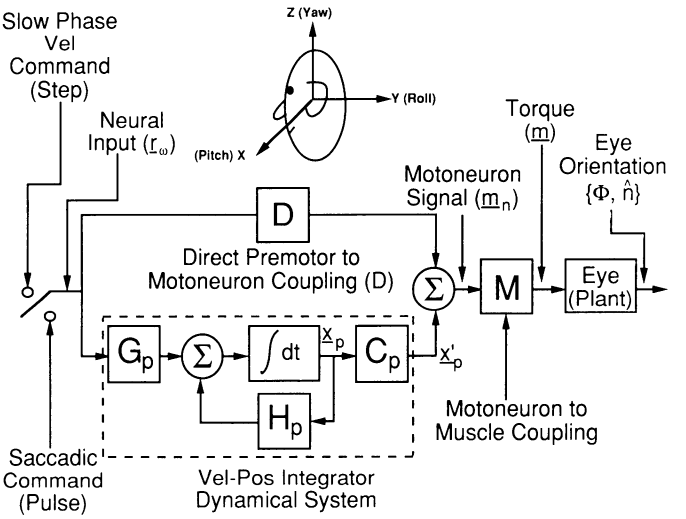

FIG. 1. Three-dimensional model of eye movement control mechanism. It is comprised of a direct premotor-to-motoneuron coupling, velocity-position dynamic system, motoneuron-to-muscle coupling, and the eye (plant). The input to the system, denoted by Neural Input, is either a slow phase velocity command (Step) or a saccadic command (Pulse), with coupling matrix G_p. The direct premotor-to-motoneuron coupling is a 3×3 matrix, D. The velocity-position integrator is a 3-dimensional extension of the 1-dimensional neural integrator. The dynamics of the integrator are governed by 3 operators, G_p, C_p, and H_p. The eigenvalues of H_p determine the time constants of the velocity-position integrator, whereas G_p and C_p are the input coupling and output coupling, respectively. The output of the integrator sums with the output of the direct premotor-to-motoneuron path to generate the motoneuron signal. The motoneuron signal drives the muscles, through matrix M, generating the torque to orient the eye (plant). See text for values of the elements of the various matrices. The drawing above the model shows the head fixed coordinate system used in this study.

the orientation of the eyes during periods of fixation or for input frequencies well below the reciprocal of the dominant time constant of the eye plant.

An important aspect of the model is that all signals up to and including the torque are neural vector signals. The operators G_p, C_p, and H_p associated with the velocity-position integrator, as well as D, associated with direct premotor-to-motoneuron coupling, are vector transformations on the neural vector signals. The transformation M transduces the neural vector signals to torque vectors generated by the eye muscles. Thus all signals obey rules of commutativity associated with vector addition. On the other hand, eye orientation does not obey the rules of commutativity for rotations of the eye and cannot be represented by a vector. Thus the eye plant dynamical system in three dimensions is an important dynamic transformation that must convert torque, which is a vector, to orientation, which is not a vector. Models that do not consider the torque-orientation relationship of the eye cannot appropriately model the velocity-position integrator in three dimensions and must resort to nonphysiological representations (Hepp and Henn 1987; Tweed and Vilis 1987). We now show how a unique torque-orientation transformation can be obtained in three dimensions that will govern the dynamics of eye rotations in response to an applied torque.

Torque-orientation relationship for eye rotations

In one dimension the orientation of the eye is given as a position relative to the midposition. When the eye is moved there is a restoring torque developed that can be given by

$$T(\Phi) = -K\Phi \tag{1}$$

where $T(\Phi)$ is the restoring torque, Φ is the angular position change from midposition, and K is the effective elasticity constant associated with tissues surrounding the eye such as Tenon's capsule, optic nerve, and suspensory ligaments (Robinson 1975b). Thus the function T versus Φ represents the torque-orientation relation for eye rotations in one dimension. If the applied torque that positions the eye were suddenly removed, the eye would return to midposition with the torque declining linearly as a function of Φ (*Eq. 1*).

In three dimensions the orientation of the eye in the head cannot be represented by a vector. It can be described by a wide range of parameters that are defined by the Fick, Helmholtz, and Listing systems (Collewijn et al. 1988; Hepp et al. 1989; Nakayama and Balliet 1977; Robinson 1975b). Orientations in the Fick and Helmholtz systems are special cases of an Euler angle system that uniquely defines the orientation relative to a primary orientation (Goldstein 1980; Pio 1966). One Euler system, referred to as the Fick system (Fig. 2*A*), gives eye orientation by a rotation, ϕ, about a space vertical axis (z), a rotation about an intermediary pitch axis, θ, and a rotation about the eye roll axis, ψ. The orientation can be represented as a rotation from a primary position by a 3×3 matrix, R, whose elements are functions of the Euler parameters (See matrix of Fig. 2*A*). As the eye moves the Euler parameters change and consequently the components of the matrix change with time.

Euler's theorem (Goldstein 1980) states that any orientation of a rigid body with one point fixed can be achieved by a single rotation about an axis along a vector, $\hat{\mathbf{n}}$ through a positive angle, Φ (Fig. 2*B*). Thus $\hat{\mathbf{n}}$ defines the axis of a cone and the optic axis lies on its surface. This is also referred to as the axis-angle form for the representation of the rotation. Because the eye rotates in three dimensions, the orientation matrix, R, changes with time and can be represented in its most general form as

$$R(t) = \begin{pmatrix} a_{11}(t) & a_{12}(t) & a_{13}(t) \\ a_{21}(t) & a_{22}(t) & a_{23}(t) \\ a_{31}(t) & a_{32}(t) & a_{33}(t) \end{pmatrix} \tag{2}$$

The angle, Φ, is related to the trace of the matrix as follows (Goldstein 1980)

$$1 + 2\cos(\Phi) = tr(R) \tag{3}$$

where tr is the trace operator defined by

$$tr(R) = \sum_{i=1}^{3} a_{ii} \tag{4}$$

The vector, $\hat{\mathbf{n}}$, is unaltered by R. Therefore $\hat{\mathbf{n}}$ is an eigenvector of the rotation matrix R having an eigenvalue of unity, given by

$$R\hat{\mathbf{n}} = \hat{\mathbf{n}}. \tag{5}$$

The relationships given by *Eq. 2–5* show how Φ and $\hat{\mathbf{n}}$ can be obtained from any matrix representing a rotation of the eye at any time.

Similarly, the rotation matrix, $R(t)$, can be given as

$$R(t) = [\mathbf{u}_1(t), \mathbf{u}_2(t), \mathbf{u}_3(t)] \tag{6}$$

where the column vectors, $\mathbf{u}_i(t)$, for $i = 1, 2$, and 3, can be expressed in terms of the rotation angle, $\Phi(t)$, and the axis of rotation, $\hat{\mathbf{n}}(t)$, by using the finite rotation formula (Goldstein 1980)

$$\mathbf{u}_i = \mathbf{e}_i \cos(\Phi) + \hat{\mathbf{n}} n_i [1 - \cos(\Phi)] + (\hat{\mathbf{n}} \wedge \mathbf{e}_i) \sin(\Phi) \tag{7}$$

where $\wedge$ represents the vector cross product, and

$$\mathbf{e}_1 = \begin{pmatrix} 1 \\ 0 \\ 0 \end{pmatrix}, \quad \mathbf{e}_2 = \begin{pmatrix} 0 \\ 1 \\ 0 \end{pmatrix}, \quad \mathbf{e}_3 = \begin{pmatrix} 0 \\ 0 \\ 1 \end{pmatrix} \tag{8}$$

are, respectively, the unit vectors associated with the pitch, roll, and yaw axes of the head-based coordinate system. The parameters n_1, n_2, and n_3 are respectively the pitch, roll, and yaw direction cosines of the axis of rotation relative to the head-based coordinate frame given by

$$n_i = \langle \hat{\mathbf{n}}, \mathbf{e}_i \rangle \quad i = 1, 2, 3 \tag{9}$$

The notation $\langle , \rangle$ represents the usual inner product operator.

The rotation represented by axis-angle $\hat{\mathbf{n}}(t)$ and $\Phi(t)$ specifies a unique rotation matrix, $R(t)$. Thus there is a one-to-one mapping between the matrix and axis-angle representations of the rotation (Goldstein 1980).

A particularly important aspect of the axis-angle representation is that it represents the shortest path that takes the eye from the primary orientation to a given orientation (Nakayama 1978; Nakayama and Balliet 1977). Thus, if the drive on the eye were suddenly removed, it is reasonable to expect that the restoring torque should be along the axis defined by Euler's theorem because it is the optimal path for returning the eye to the primary orientation. Therefore the restoring torque as a function of R can be chosen as proportional to the axis-angle representation of orientation. That is

$$\mathbf{T}(R) = -K\Phi(R)\hat{\mathbf{n}}(R) \tag{10}$$

The relationship between axis-angle representation for orientation and the restoring torque gives a unique torque-orientation relationship used for describing eye orientation in three dimensions. *Equation 1* for one-dimensional eye rotations is a special case of *Eq. 10* where the axis of rotation remains fixed. The form of the restoring torque as given by *Eq. 10* implies that the spring constants for rotations about pitch, roll, and yaw are equal. If they were not equal, the restoring torque would be a more complicated function of orientation. In the derivation of the dynamical system for this general case, the restoring torque would be represented as $\mathbf{T}(\Phi,\hat{\mathbf{n}})$ without utilizing *Eq. 10*. The derivation presented would otherwise be unaltered. A key nontrivial problem for the model simulation would be to derive the torque-orientation relationship using experimental data.

We now consider how the torque-orientation relation given by *Eq. 10* can be used to derive the dynamical system governing eye motion in three dimensions in response to a driving torque.

Three-dimensional formulation of eye dynamics

In one dimension, the relationship between the applied torque and the eye orientation is given by

$$m = \frac{d(J\omega_e)}{dt} + B\omega - T(\Phi) \tag{11}$$

where m is the applied torque of the muscles to the eye, J is the moment of inertia of the globe about the axis of rota-

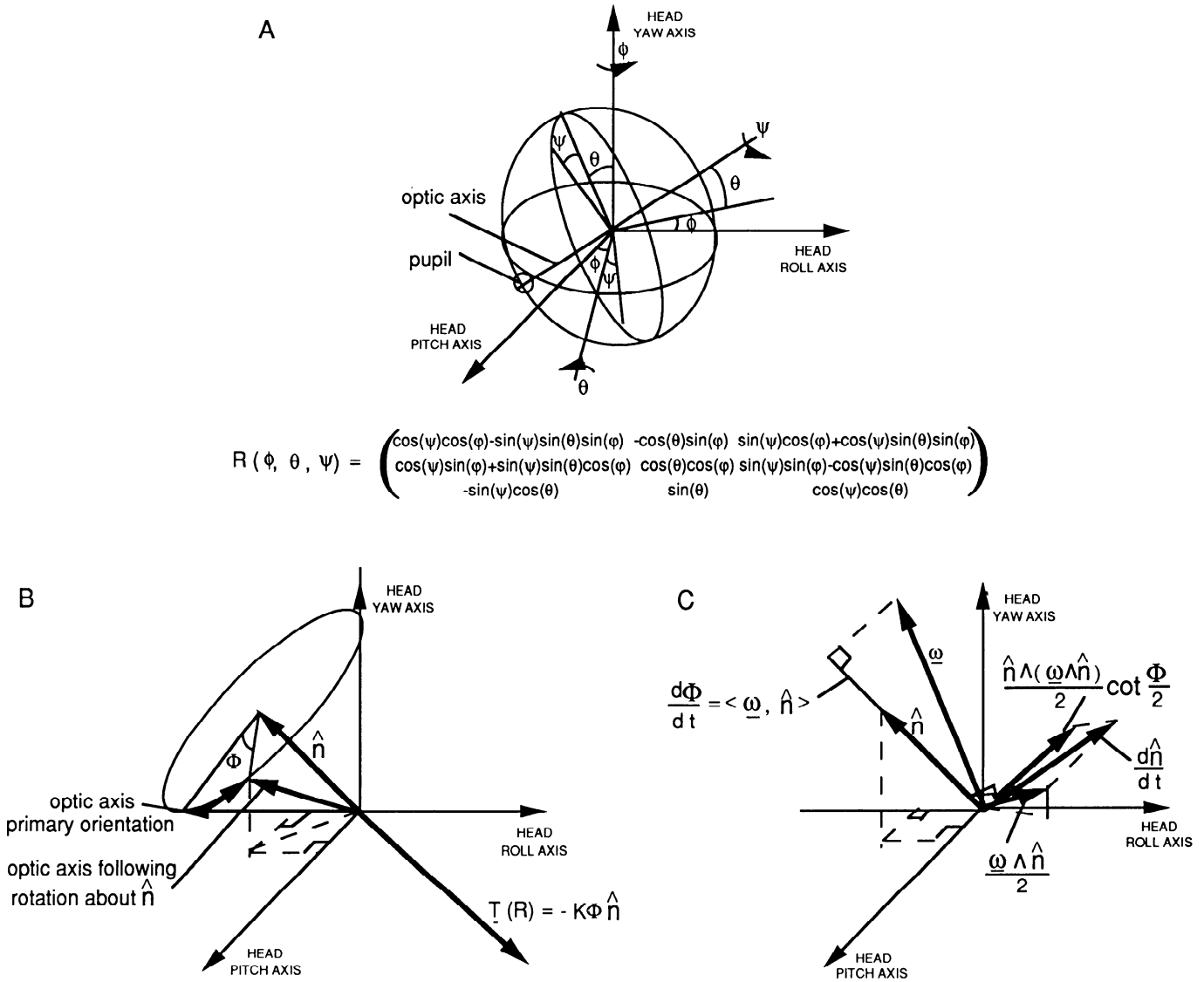

FIG. 2. *A*: orientation of eye relative to the head in terms of Fick angles. Any orientation of the eye can be given as a rotation ϕ about the fixed head yaw axis, a rotation θ about the rotated pitch axis, and a rotation ψ about the optic axis. $R(\phi,\theta,\psi)$ is the matrix representing the rotation. *B*: relationship of torque and orientation using Euler's theorem. The orientation given by matrix R (A) can also be described as a rotation about an axis along unit vector $\hat{n}$, by an angle Φ. The restoring torque, $\mathbf{T}(R)$, is given as a vector that is opposite to the vector along the axis of orientation. The magnitude of the torque is proportional to the angle of orientation, Φ. Thus $\mathbf{T}(R) = -K\Phi\hat{n}$. *C*: vector diagrams showing $d\Phi/dt$ as a projection of eye velocity onto $\hat{n}$. $d\hat{n}/dt$ is a weighted sum of 2 vectors. The weights are functions of the angle Φ and the angular eye velocity component perpendicular to $\hat{n}$. The rate of change of $\hat{n}$ is perpendicular to $\hat{n}$, as expected.

tion, B is the coefficient of viscosity, and $T(\Phi)$ is the restoring torque given by *Eq. 1*. The variables ω_e and ω are the eye velocities relative to space and to the head, respectively. $B\omega$ is the torque corresponding to the viscous damping as the eye moves in the orbit.

Equation 11 can be generalized to three dimensions as follows

$$\mathbf{m} = \frac{d(J\omega_e)}{dt} + B\omega - \mathbf{T}(R) \qquad (12)$$

where $\mathbf{m}$ is the applied torque, J is the moment of inertia tensor (Goldstein 1980), B is a matrix representing the viscous damping, ω_e and ω are the angular velocity vectors of the eye relative to space and the head, respectively, and R is a matrix representing the orientation of the eye in the head (Fig. 2*A*). Substituting *Eq. 10* into *Eq. 12* gives

$$\mathbf{m} = \frac{d(J\omega_e)}{dt} + B\omega + K\Phi\hat{n} \qquad (13)$$

Assuming that the moment of inertia of the eye in the space coordinate system is constant and proportional to the identity matrix, the dynamical system governing the eye (plant) dynamics can be given by the following formula

$$\frac{d\omega}{dt} = -J^{-1}(B\omega + K\Phi\hat{n}) - \frac{d\omega_h}{dt} + J^{-1}\mathbf{m} \qquad (14)$$

where ω_h is the angular velocity of the head relative to space and $\omega = \omega_e - \omega_h$ is the eye velocity relative to the head. *Equation 14* describes how the eye velocity vector relative to the head changes as a function of eye velocity in the head, eye orientation, head velocity in space, and applied torque. However, the eye orientation parameters, Φ and $\hat{n}$, vary

with time as the globe is rotating. Therefore equations that update the orientation parameters as a function of orientation and eye velocity relative to the head must be derived. The main results of the derivations are contained in the section entitled *Dynamical system representing the eye globe.*

Derivation of the rate of change of Φ $(d\Phi/dt)$

Our aim is to obtain a simple formula for the rate of change of Φ, $d\Phi/dt$, as a function of eye velocity in the head. We start by differentiating *Eq. 3,* which relates Φ to the rotation matrix

$$-2\sin(\Phi)\frac{d\Phi}{dt} = tr\left(\frac{dR}{dt}\right) \tag{15}$$

By combining *Eq. 15* and *Eq.* A*8* of *Appendix A* we obtain

$$-2\sin(\Phi)\frac{d\Phi}{dt} = tr(\Omega R) \tag{16}$$

where Ω is a velocity matrix operator on orientation (*Appendix A*). By combining *Eq. 4* and *16* and *Eq.* A*11* of *Appendix A* we obtain

$$-2\sin(\Phi)\frac{d\Phi}{dt} = \sum_{i=1}^{3}[\omega\wedge\mathbf{u}_i(t)]_i \tag{17}$$

We now simplify the right side of *Eq. 17.* Using the finite rotation formula, *Eq. 7,* the i^{th} vector cross product term of *Eq. 17* is

$$\omega\wedge\mathbf{u}_i = \omega\wedge\mathbf{e}_i\cos(\Phi) + \omega\wedge\hat{\mathbf{n}}n_i[1-\cos(\Phi)] + \omega\wedge(\hat{\mathbf{n}}\wedge\mathbf{e}_i)\sin(\Phi) \tag{18}$$

Utilizing the following vector identity

$$\mathbf{A}\wedge(\mathbf{B}\wedge\mathbf{C}) = \mathbf{B}\langle\mathbf{A},\mathbf{C}\rangle - \mathbf{C}\langle\mathbf{A},\mathbf{B}\rangle \tag{19}$$

the i^{th} component of $\omega\wedge\mathbf{u}_i$, i.e., $(\omega\wedge\mathbf{u}_i)_i = \langle\omega\wedge\mathbf{u}_i,\mathbf{e}_i\rangle$ can be obtained as follows

$$(\omega\wedge\mathbf{u}_i)_i = (\omega\wedge\hat{\mathbf{n}})_i n_i[1-\cos(\Phi)] + [n_i\omega_i - \langle\omega,\hat{\mathbf{n}}\rangle]\sin(\Phi), \tag{20}$$

where

$$\omega_i = \langle\omega,\mathbf{e}_i\rangle \tag{21}$$

Combining *Eq. 17* and *20* and using the identity

$$\langle\mathbf{A}\wedge\mathbf{B},\mathbf{B}\rangle = 0 \tag{22}$$

and after some simplification, we obtain the desired expression for the rate of change of Φ

$$\frac{d\Phi}{dt}\sin(\Phi) = \langle\omega,\hat{\mathbf{n}}\rangle\sin(\Phi) \tag{23}$$

For $\Phi = 0$, $\hat{\mathbf{n}}$ is undefined and *Eq. 23* is not applicable. However, $\hat{\mathbf{n}}$ can be chosen along the angular velocity vector, ω, with $d\Phi/dt$ as the magnitude of ω. For $\Phi \neq 0$, *Eq. 23* can be divided by $\sin(\Phi)$ to obtain a dynamic equation

$$\frac{d\Phi}{dt} = \langle\omega,\hat{\mathbf{n}}\rangle \tag{24}$$

This equation expresses the intuitively appealing idea that the angular rate of change of eye rotation about $\hat{\mathbf{n}}$ is the projection of instantaneous eye velocity onto $\hat{\mathbf{n}}$ (Fig. 2*C*).

Derivation of the rate of change of $\hat{n}$ $(d\hat{n}/dt)$

A similar equation for the unit vector $\hat{\mathbf{n}}$ can be derived by differentiating *Eq. 5* to obtain

$$\frac{dR}{dt}\hat{\mathbf{n}} + R\frac{d\hat{\mathbf{n}}}{dt} = \frac{d\hat{\mathbf{n}}}{dt} \tag{25}$$

Thus *Eq. 25* implicitly gives the rate of change of the orientation parameter, $\hat{\mathbf{n}}$, as a function of the rotation matrix and its derivative.

Next we find an expression for $d\hat{\mathbf{n}}/dt$ due to the eye velocity in the head, ω. Combining *Eq. 5* and *Eq.* A*8* and A*9* of *Appendix A* and substituting into *Eq. 25* we obtain

$$\omega\wedge\hat{\mathbf{n}} + R\frac{d\hat{\mathbf{n}}}{dt} = \frac{d\hat{\mathbf{n}}}{dt} \tag{26}$$

If we now find a suitable expression for $Rd\hat{\mathbf{n}}/dt$, then $d\hat{\mathbf{n}}/dt$ is determined. To accomplish this, we use the finite rotation formula for rotating $d\hat{\mathbf{n}}/dt$ (Goldstein 1980)

$$R\frac{d\hat{\mathbf{n}}}{dt} = \frac{d\hat{\mathbf{n}}}{dt}\cos(\Phi) + \hat{\mathbf{n}}\left\langle\hat{\mathbf{n}},\frac{d\hat{\mathbf{n}}}{dt}\right\rangle[1-\cos(\Phi)] + \hat{\mathbf{n}}\wedge\frac{d\hat{\mathbf{n}}}{dt}\sin(\Phi) \tag{27}$$

Because $\hat{\mathbf{n}}(t)$ is a unit vector the following relationships hold

$$\langle\hat{\mathbf{n}},\hat{\mathbf{n}}\rangle = 1$$
$$\left\langle\frac{d\hat{\mathbf{n}}}{dt},\hat{\mathbf{n}}\right\rangle = 0 \tag{28}$$

Substituting *Eq. 27* and *28* into *Eq. 26* and simplifying, we obtain

$$\omega\wedge\hat{\mathbf{n}} + \frac{d\hat{\mathbf{n}}}{dt}\cos(\Phi) + \hat{\mathbf{n}}\wedge\frac{d\hat{\mathbf{n}}}{dt}\sin(\Phi) = \frac{d\hat{\mathbf{n}}}{dt} \tag{29}$$

Next we eliminate the vector cross-product of $\hat{\mathbf{n}}$ with $d\hat{\mathbf{n}}/dt$. Because *Eq. 19* converts vector cross-products into inner products, we first take the vector cross-product of $\hat{\mathbf{n}}$ with *Eq. 29,* obtaining

$$\hat{\mathbf{n}}\wedge(\omega\wedge\hat{\mathbf{n}}) + \hat{\mathbf{n}}\wedge\frac{d\hat{\mathbf{n}}}{dt}\cos(\Phi) + \hat{\mathbf{n}}\wedge\left(\hat{\mathbf{n}}\wedge\frac{d\hat{\mathbf{n}}}{dt}\right)\sin(\Phi) = \hat{\mathbf{n}}\wedge\frac{d\hat{\mathbf{n}}}{dt} \tag{30}$$

Using *Eq. 19* and *28, Eq. 30* can be simplified as follows

$$\hat{\mathbf{n}}\wedge(\omega\wedge\hat{\mathbf{n}}) + \hat{\mathbf{n}}\wedge\frac{d\hat{\mathbf{n}}}{dt}\cos(\Phi) - \frac{d\hat{\mathbf{n}}}{dt}\sin(\Phi) = \hat{\mathbf{n}}\wedge\frac{d\hat{\mathbf{n}}}{dt} \tag{31}$$

Rearranging the terms in *Eq. 29* and *31* we obtain, respectively

$$\omega\wedge\hat{\mathbf{n}} + \hat{\mathbf{n}}\wedge\frac{d\hat{\mathbf{n}}}{dt}\sin(\Phi) = \frac{d\hat{\mathbf{n}}}{dt}[1-\cos(\Phi)] \tag{32}$$

and

$$\hat{\mathbf{n}}\wedge(\omega\wedge\hat{\mathbf{n}}) - \hat{\mathbf{n}}\wedge\frac{d\hat{\mathbf{n}}}{dt}[1-\cos(\Phi)] = \frac{d\hat{\mathbf{n}}}{dt}\sin(\Phi). \tag{33}$$

Using the trigonometric identities

$$2\sin^2\left(\frac{A}{2}\right) = 1-\cos(A) \tag{34}$$

and

$$\sin(A) = 2\sin\left(\frac{A}{2}\right)\cos\left(\frac{A}{2}\right) \tag{35}$$

Equations 32 and *33* can be expressed as

$$\omega\wedge\hat{\mathbf{n}} + 2\left(\hat{\mathbf{n}}\wedge\frac{d\hat{\mathbf{n}}}{dt}\right)\sin\left(\frac{\Phi}{2}\right)\cos\left(\frac{\Phi}{2}\right) = 2\frac{d\hat{\mathbf{n}}}{dt}\sin^2\left(\frac{\Phi}{2}\right) \tag{36}$$

and

$$\hat{\mathbf{n}}\wedge(\omega\wedge\hat{\mathbf{n}}) - 2\hat{\mathbf{n}}\wedge\frac{d\hat{\mathbf{n}}}{dt}\sin^2\left(\frac{\Phi}{2}\right) = 2\frac{d\hat{\mathbf{n}}}{dt}\sin\left(\frac{\Phi}{2}\right)\cos\left(\frac{\Phi}{2}\right) \tag{37}$$

By multiplying *Eq. 36* by $\sin(\Phi/2)$ and *Eq. 37* by $\cos(\Phi/2)$ and then adding and simplifying the resulting equations, we obtain

$$\frac{d\hat{n}}{dt}\sin\left(\frac{\Phi}{2}\right) = \frac{\omega\wedge\hat{n}}{2}\sin\left(\frac{\Phi}{2}\right) + \frac{\hat{n}\wedge(\omega\wedge\hat{n})}{2}\cos\left(\frac{\Phi}{2}\right) \quad (38)$$

For $\Phi = 0$, $\hat{n}$ is undefined and *Eq. 38* is not applicable. The vector $\hat{n}$ can therefore be chosen along the angular velocity vector, ω, with $d\Phi/dt$ as the magnitude of ω. For $\Phi \neq 0$, *Eq. 38* can be divided by $\sin(\Phi/2)$ to obtain a dynamic equation for $d\hat{n}/dt$ given by

$$\frac{d\hat{n}}{dt} = \frac{\omega\wedge\hat{n}}{2} + \frac{\hat{n}\wedge(\omega\wedge\hat{n})}{2}\cot\left(\frac{\Phi}{2}\right) \quad (39)$$

The components contributing to the rate of change of $\hat{n}$ are a weighted sum of vectors perpendicular to $\hat{n}$ (Fig. 2*C*). The weights are functions of the angle Φ and the angular eye velocity component perpendicular to $\hat{n}$. The rate of change of $\hat{n}$ is perpendicular to $\hat{n}$, as expected. This is in contrast to the manner in which Φ changes, being only dependent on the component of eye velocity along $\hat{n}$.

Dynamical system representing the eye globe

The dynamical system representing how eye orientation changes in response to an applied torque can now be given by the combined *Eq. 14, 24,* and *39*

$$\begin{aligned}\frac{d\omega}{dt} &= -J^{-1}(B\omega + K\Phi\hat{n}) - \frac{d\omega_h}{dt} + J^{-1}\mathbf{m}\\ \frac{d\Phi}{dt} &= \langle\omega, \hat{n}\rangle,\\ \frac{d\hat{n}}{dt} &= \frac{\omega\wedge\hat{n}}{2} + \frac{\hat{n}\wedge(\omega\wedge\hat{n})}{2}\cot\left(\frac{\Phi}{2}\right)\end{aligned} \quad (40)$$

where ω is the angular velocity of the eye with respect to the head, ω_h is the angular velocity of the head with respect to space, Φ and $\hat{n}$ represent the orientation of the eye with respect to the head, $\langle,\rangle$ is the inner product operator, and $\wedge$ is the vector cross product operator. In this form, the rates of change of the variables of interest are given in terms of their values and applied torque at any time, t. This allows the computation of the values of the variables at time $t + dt$. Thus the equations can be integrated computationally for any applied torque for purposes of simulation. We now consider how the torque is generated centrally.

Modeling the velocity-position integrator

In the present conceptual framework, the velocity-position integrator is a dynamical system that transforms neural signals representing an angular velocity command to a state that is linearly related to torque. Thus the integrator will be given by (Fig. 1)

$$\begin{aligned}\frac{d\mathbf{x}_p}{dt} &= H_p\mathbf{x}_p + G_p\mathbf{r}_\omega\\ \mathbf{m}_n &= C_p\mathbf{x}_p + D\mathbf{r}_\omega\end{aligned} \quad (41)$$

where H_p is the system matrix for the velocity-position integrator and G_p is the coupling to the integrator from a neural signal coding the eye velocity command, $\mathbf{r}_\omega$. The matrices C_p and D transform the state of the integrator and command velocity to a signal, $\mathbf{m}_n$. The matrix D may depend on whether it is activated by a slow phase velocity or saccadic command. In the simulations it was held constant. The output, $\mathbf{m}_n$, is a superposition of the state of the velocity-position integrator, $\mathbf{x}_p$, and the direct premotor-to-motor coupling signal. The signal, $\mathbf{m}_n$, is transduced into a torque by the muscles, represented by matrix M, where

$$\mathbf{m} = M\mathbf{m}_n \quad (42)$$

The concatenation of the system given by *Eq. 41* and *42* with that given by *Eq. 40* describes the dynamics and kinematics of rotations in three dimensions due to a neural "velocity command" signal. Thus all the central signals are vectors and naturally have commutative properties, whereas the dynamics of the plant convert the applied torque vector into an eye orientation trajectory over time.

Model simulations

To simulate eye orientation from activation of a velocity-position integrator, *Eq. 41* was coupled to *Eq. 40* by a linear equation (*Eq. 42*). We then activated the velocity-position integrator with pulses and steps, signals that have been closely linked to saccadic and smooth pursuit behavior. We wish to demonstrate that the proposed model that incorporates a generalization of the one-dimensional integrator (Skavenski and Robinson 1973), together with the appropriate three-dimensional model of the plant, can simulate the kinematic rotation properties and the dynamic properties of eye movements. The dynamic aspects of the eye movements have been virtually ignored in present three-dimensional models of eye rotation (Tweed and Vilis 1987).

In the simulations we neglected the muscle mass and the dependence of muscle tension on muscle length. It was also assumed that there was a linear dependence of tension in a muscle on its innervation and that the tension was independent of changes in eye orientation due to innervation of other muscles. The inertia tensor, J, and damping matrix, B, were chosen proportionally to the identity matrix given by

$$\begin{aligned}J &= 5\times10^{-7}\ \text{kg}\cdot\text{m}^2\begin{bmatrix}1&0&0\\0&1&0\\0&0&1\end{bmatrix}\\ B &= 7.476\times10^{-5}\ \text{kg}\cdot\text{m}^2/\text{s/rad}\begin{bmatrix}1&0&0\\0&1&0\\0&0&1\end{bmatrix}\end{aligned} \quad (43)$$

Therefore the moment of inertia and damping about any axis of rotation were constant. The ratio of the "spring constant", K, to the moment of inertia was chosen as 952.4 s^{-2}/rad and the ratio of the damping coefficient to moment of inertia was chosen as 149.5 s^{-1}/rad (*Eq. 40*). These values were chosen to correspond to the approximate dominant time constants associated with the eye plant of 0.15 and 0.007 s (Robinson et al. 1969). The matrices H_p, G_p, C_p, and D, associated with the velocity-position integrator, were chosen as diagonal and are given as

$$H_p = -0.03333\begin{bmatrix}1&0&0\\0&1&0\\0&0&1\end{bmatrix}$$

$$G_p = 0.3333\begin{bmatrix}1&0&0\\0&1&0\\0&0&1\end{bmatrix} \qquad (44)$$

$$C_p = 29.44\begin{bmatrix}1&0&0\\0&1&0\\0&0&1\end{bmatrix}$$

$$D = 0.1389\begin{bmatrix}1&0&0\\0&1&0\\0&0&1\end{bmatrix}$$

The values of the matrix parameters were picked to obtain states of the velocity-position integrator to match the approximate orientation of the eye in steady state. The three eigenvalues of H_p were chosen to correspond with 30-s time constants, consistent with the long time constant of velocity-position integration. Different values could be chosen along the diagonal of H_p to generate different time constants for pitch, roll, and yaw components. The coupling matrix between the neural signal and the muscle torque, M, was chosen proportional to the identity matrix

$$M = 2.493 \times 10^{-6}\,(\text{kg}\cdot\text{m}^2/\text{s}^2)/(\text{spikes/s})\begin{bmatrix}1&0&0\\0&1&0\\0&0&1\end{bmatrix} \qquad (45)$$

$MC\mathbf{x}_p$ is the torque that maintains the steady-state orientation.

Simulation of saccadic eye movements

To simulate saccadic movements, pulses representing neural burst commands were given. The duration of the pulses was chosen as 50 ms, corresponding to the duration of an average 10° saccade. The pulses were chosen to have a linear decline over their duration. This approximates the behavior of medium lead burst units in the PPRF, which are believed to drive the velocity-position integrator (Henn and Cohen 1976; Hepp and Henn 1983; Keller 1974; Luschei and Fuchs 1972; Van Gisbergen et al. 1981). The parameters associated with the integrator were chosen so that it would produce a pulse-step ratio of 3.5 to achieve pulse-step matching for correct saccade dynamics (Optican and Miles 1985; Optican and Robinson 1980) (*Appendix B*). This ratio agrees with the average pulse-step ratios reported for motoneuron firings (Fuchs and Luschei 1970, 1971; Henn and Cohen 1973; Keller and Robinson 1972).

Figure 3 shows the response of the model to a vector of pulses that produce an oblique saccade from the primary position. The pulses (Fig. 3*A*) are integrated vectorially by the velocity-position integrator (Fig. 1). Note that the state of the integrator (Fig. 3*B*) is declining after the initial rise and is dependent on the eigenvalues of the system matrix associated with the velocity-position integrator, H_p. The pulse-step is produced by a linear combination of the output of velocity position and the input pulse (Fig. 3*C*). The pulse-step generates the muscle torque to drive the eyes. In response to this torque there is a change in orientation angle about an axis whose direction cosines are constant throughout the movement (Fig. 3*D*). The apparent rapid changes

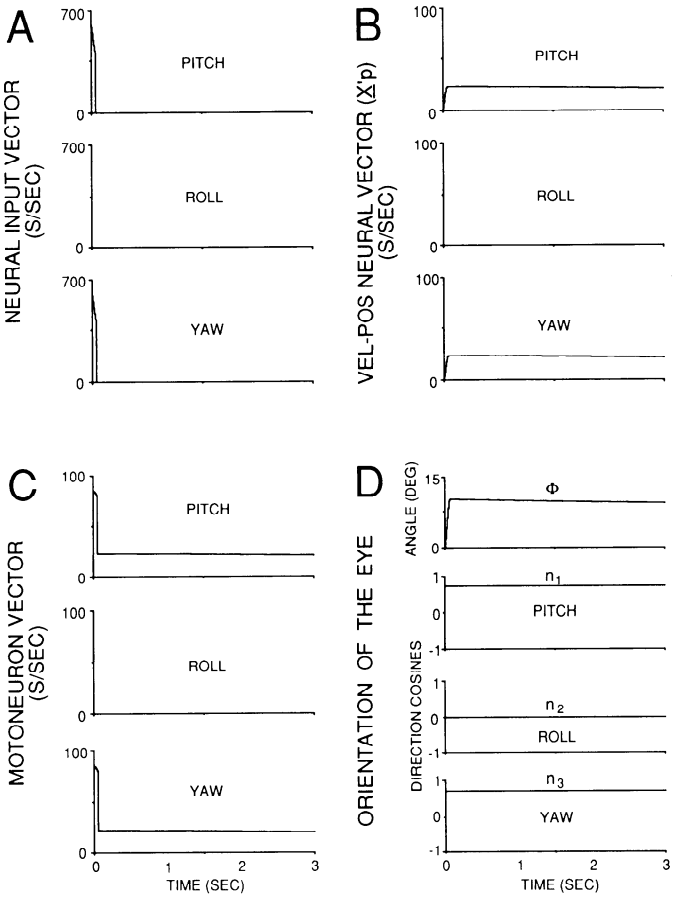

FIG. 3. Model simulation of premotor and motor neural pulses and the associated eye orientation response for a centrifugal saccadic eye movement. *A*: input neural pulse vector along the pitch-yaw direction. Neural vector components were scaled to be representative of frequency of firing (spikes/s) of premotor and motoneurons and given as spikes/s. *B*: integrator response vector is an approximate step along the pitch-yaw direction, which decays toward 0. C, The superposition of the pulse and step gives a motoneuron vector that is a pulse step also along the pitch-yaw direction. *D*: eye orientation during the eye movement. The angle of rotation is Φ; it is denoted by ANGLE (DEG). The axis about which the eye has rotated from the primary orientation is defined by DIRECTION COSINES, n_1, n_2, and n_3 along the pitch, roll, and yaw axes of the head. The variation of the ANGLE (DEG) and the DIRECTION COSINES as a function of time specify the eye orientation during its trajectory. The angle of rotation, Φ, is always positive and the direction cosines range between −1 and 1. In all subsequent figures eye orientation is similarly defined.

in the direction cosines in the simulations are due to the assumption that when the eye is in the primary position and not moving the direction cosines are 0. This indicates that from the primary position the eye can move about any axis causing a rapid jump in the direction cosines. Similar jumps in direction cosines are observed in all subsequent simulations.

The orientation angle decays back to the primary position, whereas the direction cosines remain unchanged (Fig. 3*D*). Listing's law (Haustein 1989; Hepp 1990; Hepp and Henn 1987; Tweed and Vilis 1987, 1988) is automatically obeyed because the vector associated with the pulse input is in Listing's plane, i.e., the plane formed by the pitch and yaw axes in head coordinates. A rotation of the reference axes could be implemented to place Listing's plane to correspond more exactly to physiological findings, but this would not alter the basic findings of this study.

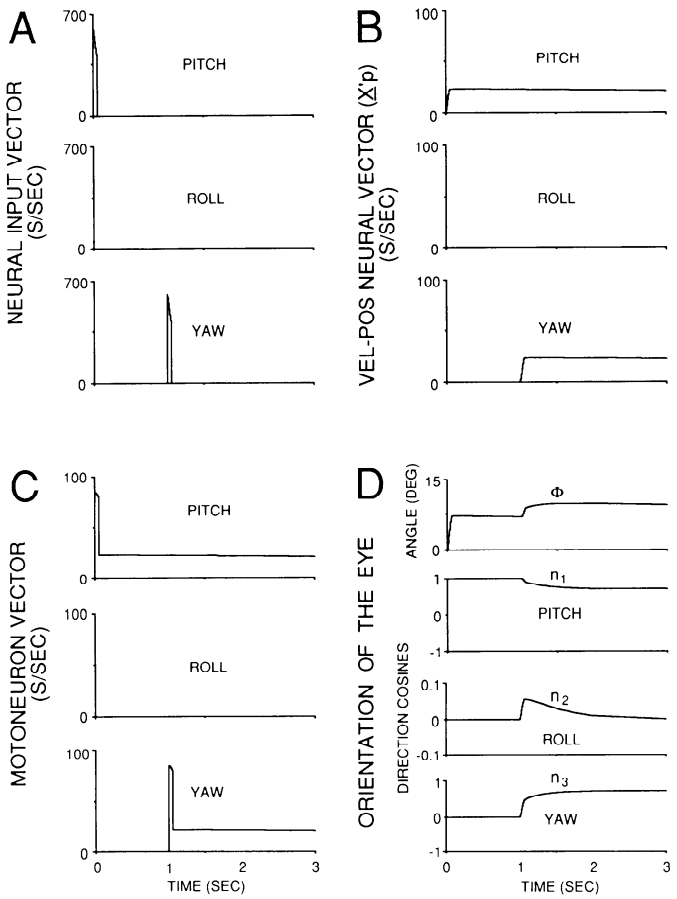

FIG. 4. *A*: model simulation of the response to a pulse input vector first along the pitch direction followed by a pulse along the yaw direction. *B*: integrator response follows the input sequence with an approximate step along the pitch direction followed by a step along the yaw direction. *C*: superposition of the pulse and step gives a motoneuron vector that is a pulse step in the same sequence. *D*: direction cosines of eye movement indicate that the orientation first changes along the pitch axis. When the yaw pulse-step activates the eye from an already pitched position, the eye orientation changes have pitch, roll, and yaw components. The roll direction cosine decays to 0, leaving only pitch and yaw components, as in Fig. 3*D*, obeying Listing's law. The angle of the eye orientation changes accordingly.

To show that the order in which the input pulses are applied to the velocity-position integrator does not matter in determining final eye orientation, pulses were applied first along the pitch axis and then the yaw axis separated by 1 s (Fig. 4*A*). This induces a change in integrator state along the pitch axis followed by a change in state along the yaw axis (Fig. 4*B*). The pulse-steps are similarly displaced (Fig. 4*C*). In response to this sequence of pulses, eye orientation changes rapidly about the pitch axis, with the direction cosines remaining constant (Fig. 4*D*). When the second pulse along the yaw axis is initiated, eye orientation and all direction cosines transiently change. However, the steady-state eye orientation angle and the direction cosines after the second pulse are approximately equal to the orientation angle and direction cosines for movement from the primary position (compare Figs. 3*D* and 4*D*). Because the simulations were performed in the dark there are negligible differences between Figs. 3*D* and 4*D* at some time after the second pulse because of the small amount of decay of the velocity-position integrator state during the period between the two pulses. Thus Listing's law is obeyed in the steady state.

If the pulses are reversed such that the yaw pulse is delivered first followed by the pitch pulse after 1 s (Fig. 5*A*) it has similar consequences. The velocity-position integrator state (Fig. 5*B*) and the pulse-step (Fig. 5*C*) that drives the eyes first change only about a yaw axis. The direction cosines remain constant. In response to the second pulse the velocity-position integrator just builds up along the pitch axis. However, eye orientation changes such that the direction cosines transiently change and approach those obtained for the change in eye orientation from the primary position (compare Figs. 3*D* and 5*D*). They also are equal to that obtained when the pitch pulse was applied first (compare Figs. 4*D* and 5*D*). This shows that commutativity holds for this system and Listing's law is obeyed in the steady state if two pulses are applied along the pitch and yaw axes in any order. As time goes on the eye orientation will decay to the primary position about this axis (Fig. 5*D*), depending on the eigenvalues of the system matrix associated with the velocity-position integrator.

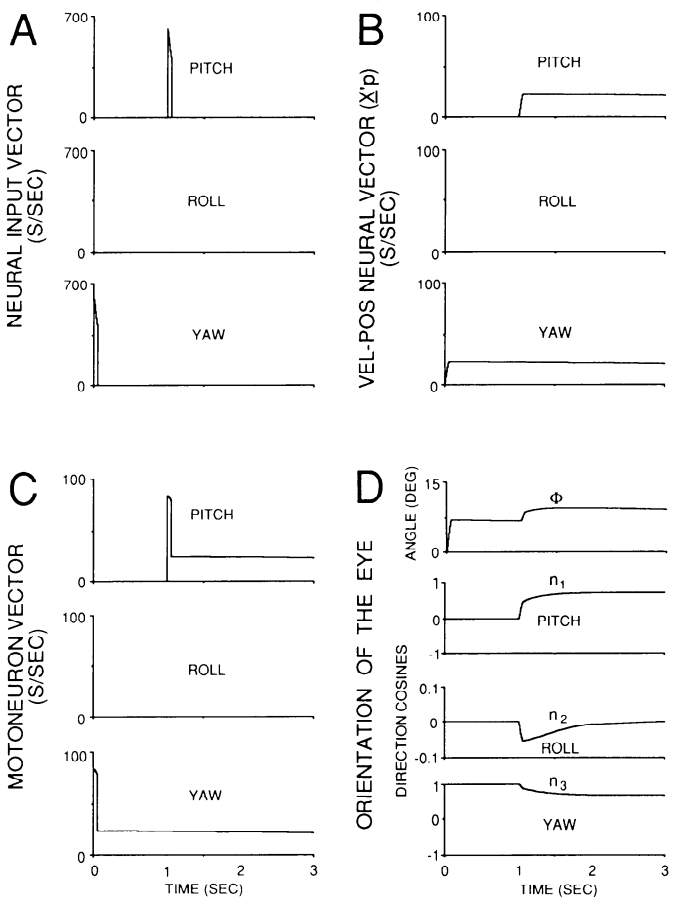

FIG. 5. *A*: model simulation of the response to a pulse input vector first along the yaw direction followed by a pulse along the pitch direction. *B*: integrator response follows the input sequence with an approximate step along the yaw direction followed by a step along the pitch direction. *C*: superposition of the pulse and step gives a motoneuron vector that is a pulse-step in the same sequence. *D*: direction cosines of eye movement indicate that the orientation first changes along the yaw axis. When the pitch pulse-step activates the eye, which is already in a yaw position, the eye orientation changes have pitch, roll, and yaw components as in Fig. 4*D*. The roll direction cosine decays to 0, leaving only pitch and yaw components as in Figs. 3*D* and 4*D* and obeying Listing's law. The angle of the eye orientation changes are as in Fig. 4*D*.

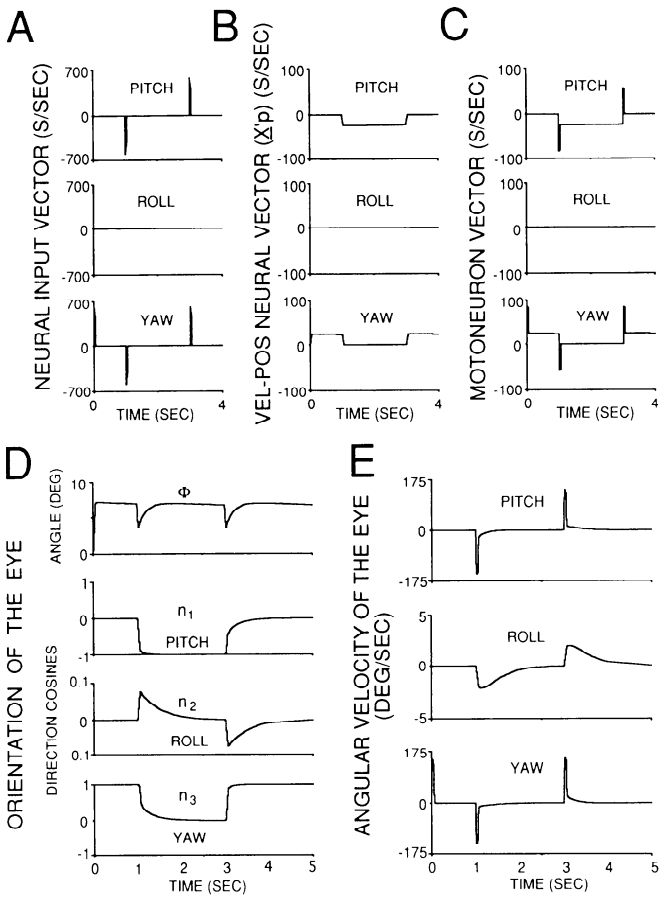

FIG. 6. Model simulations of the response to neural pulses that move the eye in a sequence that first looks left, then straight up, and then back to the left. *A*: neural input vector first has a pulse along the yaw axis. Then there are simultaneous pulses along pitch and yaw followed by simultaneous pulses along pitch and yaw in the opposite direction. The neural vector associated with the velocity-position integrator (*B*) and the motoneuron vector (*C*) follow the input, the signals being maintained along the pitch-yaw axes. The orientation of the eye (*D*) contains a direction cosine component along roll, during which time the angle decreases and increases. *E*: pitch and yaw components of the angular velocity of the eye essentially follow the pulses on the motoneuron vector. However, there is a significant roll velocity.

During the second saccade (Figs. 4*D* and 5*D*) the roll direction cosines are not 0 and therefore there is a deviation from Listing's law. However, the direction cosine of the axis reaches a maximum of <0.055 (note different scales for roll in Figs. 4*D* and 5*D*), and the average deviation from Listing's law is well within the error bounds reported in the literature (Haslwanter et al. 1992; Tweed and Vilis 1990a). It should be noted that the saccadic movement due to the second pulse is from a secondary to a tertiary eye position and the saccade trajectory appears "slow" because of the transient roll component (see DISCUSSION).

We next examine the model predictions when saccadic eye movements are made from looking left to looking straight up and then back to looking left (Fig. 6). This was done to determine to what extent Listing's law is obeyed when eye movements are made from a secondary to a tertiary position and to determine whether the model could predict data that examined the position and velocity characteristics of these types of eye movements (Tweed and Vilis 1988). The simulation begins with the eye in the primary position and a pulse 50 ms in duration is applied along the yaw axis at time $t = 0$ (Fig. 6*A*). The pulse activates the yaw state of the velocity-position integrator (Fig. 6*B*) and together they generate a pulse-step (Fig. 6*C*). The eye muscles respond to the pulse-step and generate a torque on the eye causing a leftward rotation that is held for ~1 s (Fig. 6*D*). The direction cosines for the axis of this movement are 0, 0, and 1 with an angle of 7° (Fig. 6*D*). At this time two pulses, one along the pitch axis and one along the yaw axis, are applied simultaneously (Fig. 6*A*), causing the yaw component of the velocity-position integrator state to go to 0 and the pitch component to be activated (Fig. 6*B*). The corresponding pulse-steps along the pitch and yaw axes (Fig. 6*C*) rotate the eye so that the direction cosines for pitch, roll, and yaw are −1, 0, and 0 with an angle of 7° at approximately $t = 3$ s (Fig. 6*D*). This corresponds to the eye looking upward in the steady state.

The rotation of the eye for this sequence of pulses constitutes an oblique eye movement from looking left to looking straight up. This rotates the eye clockwise about the positive roll axis. When the system is again activated by two simultaneous pulses along the pitch and yaw axes after $t = 3$ s (Fig. 6*A*) the velocity-position integrator returns to a state where only a yaw component is present (Fig. 6*B*). This again produces a pulse-step (Fig. 6*C*) bringing the eye back to a looking left position. The roll component has similar dynamic characteristics but is opposite to that when the eye moves from left to up (Fig. 6*D*).

The simulations indicate that during this oblique eye rotation there is a positive direction cosine for the roll axis that decays toward 0 over ~2 s (Fig. 6*D*). The non-0 direction cosine indicates that the axis of eye rotation deviates from Listing's plane during the movement and approaches Listing's plane in the steady state. However, the maximum deviation is <0.077 compared with a pitch direction cosine of −1. In addition, during the saccade, the angle of the rotation, Φ, drops to 4°. Thus the average deviation from Listing's plane for this case as well is within the error bounds reported in the literature.

The three-dimensional velocity plots as a function of time indicate that in addition to pitch and yaw velocities there is also a negative roll velocity that is generated during the rotation of the eye from looking left to looking straight up, i.e., up and to the right movement (Fig. 6*E*), and a positive roll velocity when the eye movement is down and to the left. These directions agree with the data on oblique eye movements for this condition (Tweed and Vilis 1988).

Because of the transient roll component that slowly decayed, the question arose as to whether the roll component would build up if saccades were made around the corners of a triangle (Nakayama 1975) every 250 ms. The required movement is from the primary orientation, looking left, left and up, and then back to the primary orientation. This was simulated by applying simultaneous pulses along pitch and yaw for three cycles (Fig. 7*A*). The velocity-position integrator state (Fig. 7*B*) and motoneuron vector (Fig. 7*C*) behave as expected, giving corresponding steps and pulse-steps. The eye orientation trajectory is shown in Fig. 7*D*. When the eye moves left the direction cosines for pitch, roll, and yaw are 0, 0, and 1 as expected. When the eye moves to the left-up orientation the direction cosines for pitch and yaw approach −0.7 and 0.7, respectively. The roll tran-

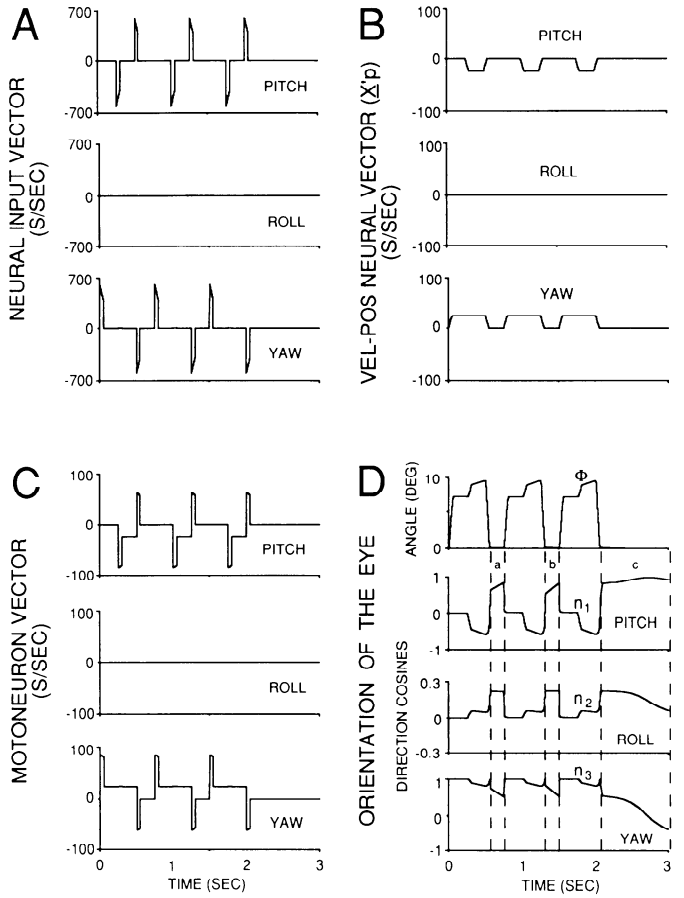

FIG. 7. Model simulation of the response to pulses that move the eye from primary position to left, left and up, and back to the primary position (*A*), according to the paradigm used by Nakayama (1975). There were induced changes in orientation every 250 ms. The integrator changes in a stepwise fashion in the pitch-yaw plane (*B*) and the motoneurons have a pulse-step also confined to the pitch-yaw plane (*C*). Eye orientation (*D*) follows the triangular motion with a small roll component when the eye moves to tertiary orientations. However, there is no sustained buildup in roll, because the eye "untwists" when returned to the primary orientation. The regions of time between the vertical dotted lines, labeled *a*, *b*, and *c*, correspond to an eye orientation extremely close to the primary position where the eye orientation angle, state of the velocity-position integrator, and eye velocity are ~0. The changes in direction cosines of the axis near this singular state do not correspond to any meaningful changes in orientation.

siently changes and then starts to decay. Before steady state is reached the simultaneous pitch and yaw pulses bring the eye back to the primary orientation as the angle goes sharply to 0 (Fig. 7*D*). In this condition the state of the velocity-position integrator, angle of eye orientation, and eye velocity are all close to 0 and represent a singular condition for the direction of the axis, $\hat{n}$, indicated by the regions *a*, *b*, and *c* between the dotted lines (Fig. 7*D*). The changes in direction cosines of the axis in these regions do not correspond to meaningful changes in orientation. Immediately after the singular portions of the trajectory, when the eye is rotated left, the pitch and roll direction cosines rapidly return to 0, whereas the yaw direction cosine is 1. This is because the eye is making a centrifugal saccade and Listing's law is obeyed throughout the trajectory (Fig. 7*D*). Thus there is no buildup of roll when the eye is moving rapidly around a triangle starting in the primary orientation.

Simulation of smooth pursuit eye movements

To simulate eye orientation response to smooth pursuit or a step in head velocity about an axis in a coronal plane, steps in the pitch and yaw components were simultaneously applied as input to the velocity-position integrator and the direct pathway (Fig. 8*A*). The step rise time was chosen as 1 ms, the iteration interval for the simulation. The step size was chosen to induce a slow phase eye velocity of ~3.5°/s so that the change in eye orientation would be approximately that obtained for the saccadic simulation; it remained well within the normal range of eye movements over a 3-s period. In response to the steps, the velocity-position integrator rises in a ramplike fashion in the two components that were excited (Fig. 8*B*). When the integrator state and direct pathway are linearly combined, the approximate step-ramp is produced (Fig. 8*C*). This signal generates the muscle torque that changes eye orientation angle approximately linearly and maintains the direction cosines constant (Fig. 8*D*). The angle of eye orientation increases linearly. The angle and direction cosines of eye orientation

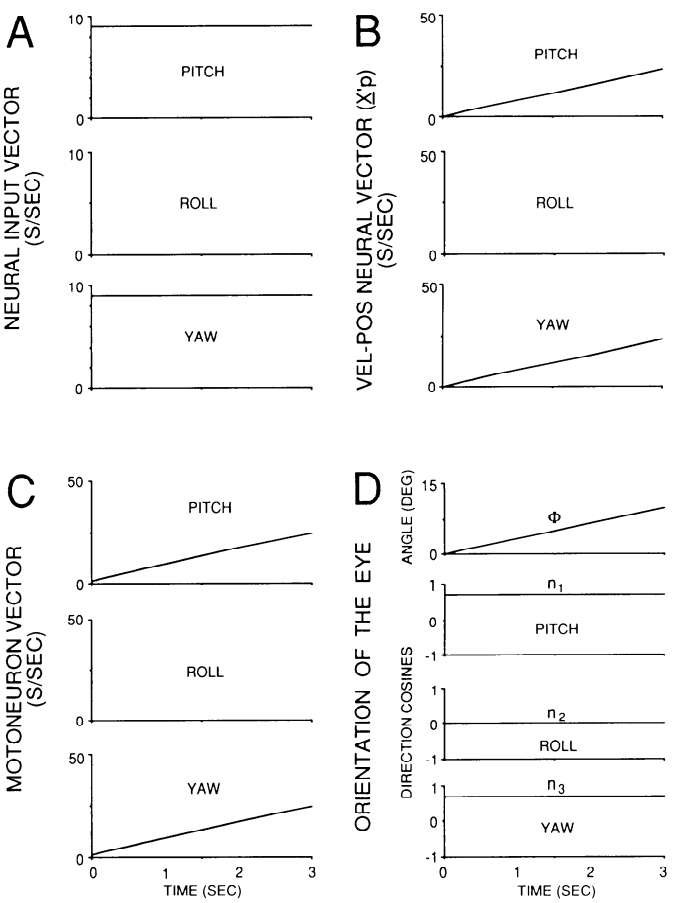

FIG. 8. *A*: model simulation of the response to a step neural input vector along the pitch-yaw direction. The integrator response (*B*) is an approximate ramp along the pitch-yaw direction. The superposition of the step and ramp gives a motoneuron vector that is a step-ramp also along the pitch-yaw direction (*C*). The step size was chosen to induce a slow phase eye velocity of ~3.5°/s so that the total eye deviation was approximately that of the simulated saccade. The speed was also slow enough so that the orientation change could be followed over 3 s and remain well within the range of normal eye movements. The eye orientation (*D*) is a centrifugal slow eye movement along the pitch-yaw axis and is aligned with the stimulus direction. The change in angle is consistent with the characteristics of a slow eye movement (ANGLE).

together indicate that a centrifugal slow eye movement along the pitch-yaw axis aligned with the stimulus direction is being executed (Fig. 8*D*).

When the step in pitch is applied followed by the step in yaw (Fig. 9*A*), the state of the velocity-position integrator rises linearly first in the pitch component followed by a linear rise in the yaw component 1 s later (Fig. 9*B*). The step-ramp components are also displaced in time (Fig. 9*C*) and produce the torque that orients the eyes. Eye orientation angle increases approximately linearly. The direction cosine of the movement associated with the pitch axis becomes 1 for 1 s, indicating a rotation of the eye about only the pitch axis (Fig. 9*D*). In response to the second step the orientation angle continues to rise approximately linearly, but the direction cosine for pitch decreases, whereas the direction cosines for roll and yaw increase (Fig. 9*D*). This indicates that the eye is changing its rotation axis while it is moving. The orientation of the eye as indicated by the direction cosines (Fig. 9*D*) is approaching the orientation of the eye for simultaneous step inputs (compare Figs. 8*D* and 9*D*).

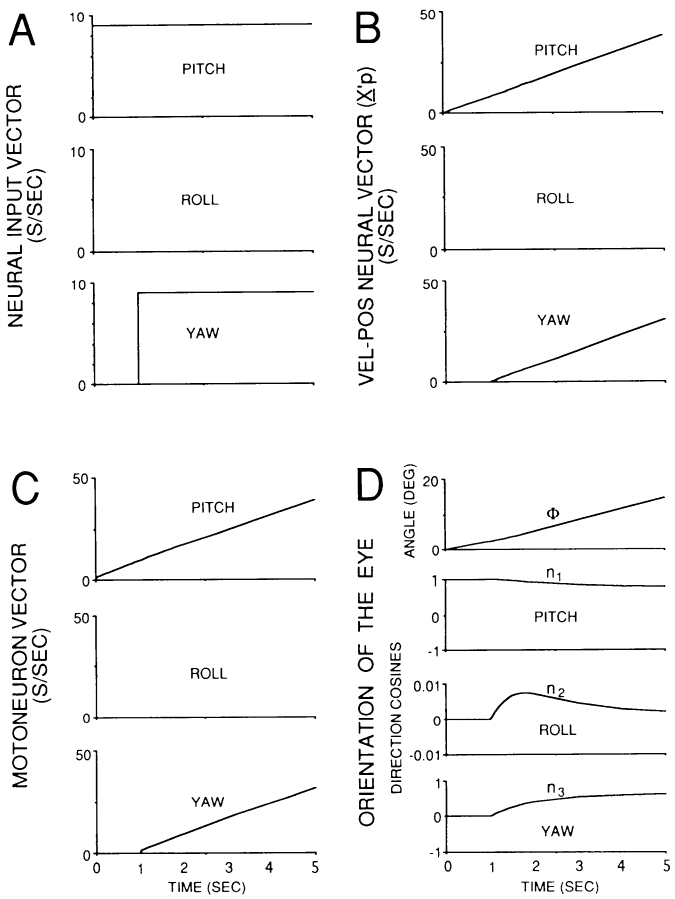

FIG. 9. Model simulation of the response to a step of neural input vector first along the pitch direction followed by a step along the yaw direction (*A*). The integrator response (*B*) follows the input sequence with an approximate ramp along the pitch direction followed by a ramp along the yaw direction. The superposition of the ramp and step gives a motoneuron vector which is a step-ramp in the same sequence (*C*). *D*: direction cosines of eye movement indicate that the orientation first changes along the pitch axis. When the yaw step ramp activates the eye from an already pitched position, the eye orientation changes have pitch, roll, and yaw components. The roll direction cosine decays to 0 over a 5 s time course, leaving only pitch and yaw components as in Fig. 8. After sustained following for >5 s, Listing's law would be obeyed.

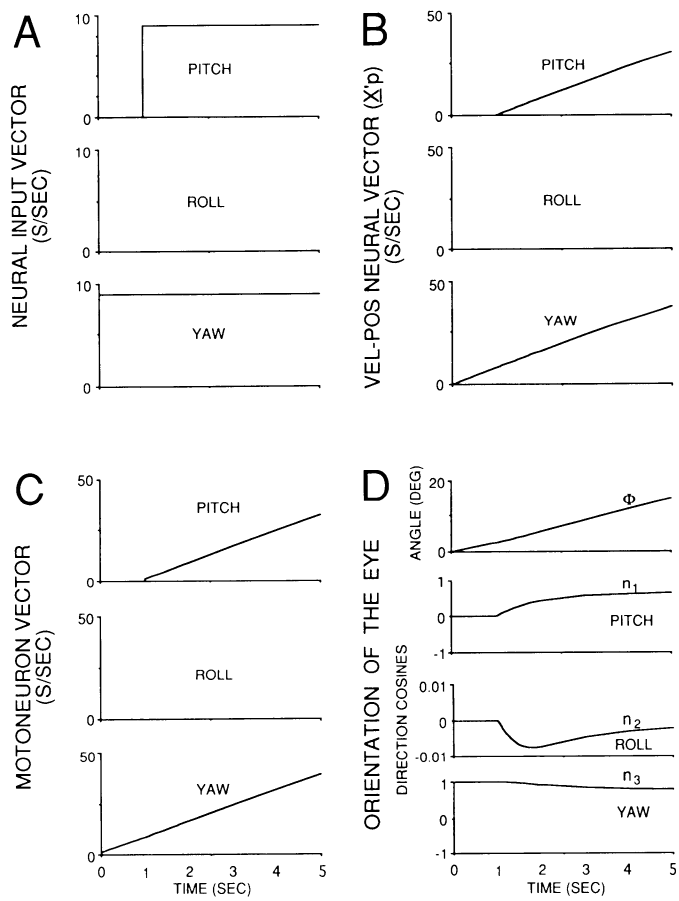

FIG. 10. Model simulation of the response to a step of neural input vector first along the yaw direction followed by a step along the pitch direction (*A*). The integrator response (*B*) follows the input sequence with an approximate ramp along the yaw direction followed by a ramp along the pitch direction. The superposition of the ramp and step gives a motoneuron vector that is a step-ramp in the same sequence (*C*). *D*: direction cosines of eye movement indicate that the orientation first changes along the yaw axis. When the pitch step ramp activates the eye from a yaw position the eye orientation changes have pitch, roll, and yaw components. The roll direction cosine decays to 0 over a 5-s time course, leaving only pitch and yaw components as in Figs. 8 and 9. After sustained following for >5 s, Listing's law would be obeyed.

When the step in yaw is applied first, followed by the step in pitch (Fig. 10*A*), the velocity-position integrator yaw component builds up linearly first, followed by a linear buildup in the pitch component after 1 s (Fig. 10*B*). The step-ramps follow the same sequence (Fig. 10*C*). Eye orientation angle again builds up approximately linearly (Fig. 10*D*). However, the direction cosines that define the orientation of the rotation axis change with time. In the limit the direction cosines of the axes of eye rotation do not depend on the order of the steps (compare Figs. 8*D*, 9*D*, and 10*D*) and commutativity holds.

The decay rates for the roll in both Figs. 9*D* and 10*D* are such that it would take ~5 s to reach equivalent orientations. Crawford and Vilis (1991) reported a steady-state roll component during a step of head velocity with the eye looking down. This buildup in the roll component and the time course of the decay to 0 in the model simulation (Fig. 9*D*) is consistent with this result. If a saccadic eye movement occurred 1 s after the head rotation, it would appear as if a steady-state roll component had developed during the slow phase (Crawford and Vilis 1991). It should be noted that

the maximum roll direction cosine is <0.008, and therefore Listing's law is obeyed throughout the trajectory.

DISCUSSION

The major conclusion of this study is that velocity-position integration in three dimensions is a simple extension of that in one dimension with the subtractive feedback of the integrator represented by a matrix rather than a single parameter, i.e., its time constant. It generates a signal related to steady-state torque and not orientation. Therefore eye orientation is critically dependent on the steady-state torque-orientation relationship associated with the eye globe and its underlying tissues. In the model the torque-orientation relationship is based on the idea that the restoring torque developed by the tissues surrounding the eye globe is approximately proportional to an angular rotation about an axis from the primary position (Miller and Robinson 1984). This concept enabled us to directly relate the restoring torque associated with the eye to parameters of orientation as defined in Euler's theorem (Goldstein 1980). Euler's theorem parameterizes orientation by an axis and an angle of rotation about that axis from some primary position. The vector representing the restoring torque was simply approximated as being proportional to the product of the angle and a unit vector along the axis. Because a rotation about the axis given by Euler's theorem is the most optimal path for returning to the primary position, it was intuitively appealing that the restoring torque should be along this direction as well as establishing a unique relationship between torque and orientation. By incorporating the torque-orientation relationship into the differential equation governing eye globe dynamics, a dynamical system was derived relating eye orientation to applied torque. The velocity-position integrator and the direct pathway around it could then be coupled to the eye globe model and a system structure obtained that could be related to physiological variables. Although the complete model system equations proved to be complicated, they could easily be programmed on a computer for simulation and testing of their predictions.

In the model simulations there were small differences between conditions when the pulses were applied together compared with when they were applied sequentially. This is because all of our simulations were performed assuming that the subject was in darkness and were performed specifically to gain better insight into the dynamic relationship between the velocity-position integrator and the orientation of the eye plant. When the eye makes an oblique saccade from the primary orientation (Fig. 3) the pulses driving the saccade are applied at the same time. They charge the integrator such that the pitch and yaw components are equal. The components then decay back to 0 together. Consequently, the eye decays to the primary orientation about the axis $\hat{n}$ with a time constant of the integrator, i.e., 30 s.

When the pulses are applied in sequence, as in Fig. 4, the pitch component of the integrator state has had a chance to decay somewhat at the time the yaw pulse activates the integrator. Consequently, the axis about which the eye will decay to the primary position will be slightly different from that in Fig. 3. A similar argument applies to the comparisons between Figs. 3 and 5. Because the time constant was chosen as 30 s and the time difference between pulses in Fig. 3 was 1 s, the difference between the direction cosines of $\hat{n}$ for Figs. 3 and 4 after the roll direction cosine has decayed is $\tan^{-1}[1-\exp(-1/30)]$. This is a 1° difference. A similar difference is obtained between the simulations in Figs. 3 and 5. If the integrator had a larger time constant the difference would be smaller while accentuated with a smaller time constant. Examining saccades after lesions that affect the time constant of the velocity-position integrator would be an interesting test of the model. For any value of time constant, however, there is a unique eye orientation for a state of the velocity-position integrator. This is determined by the balance between the applied torque and the restoring torque. In light there are additional signals from the visual system that keep the eye fixated on the target and there would be no decay of the velocity-position integrator state. Under these circumstances the orientations would be identical under all conditions and commutativity would hold exactly.

A rather surprising model prediction was the slowness of the saccades made from one tertiary position to another (Figs. 4–6). This comes about because of the necessity for there to be matching between the pulse and step that drives the saccade (Optican and Miles 1985; Optican and Robinson 1980). The pulse-step match is critically dependent on the dynamics of the eye globe and the viscoelastic properties of the surrounding tissue. When there is a mismatch the eye can undershoot, followed by a glissadic eye movement to the final position (Optican and Miles 1985; Optican and Robinson 1980) (*Appendix B*). When the three-dimensional dynamical system representing the plant is driven by a two-dimensional vector in the pitch-yaw plane in head coordinates from a secondary to a tertiary position, there is of necessity a mismatch between the plant dynamics and the pulse-step driving it. The model simulations indicate that the pulse-step mismatch of driving a system that rotates in three dimensions with a two-dimensional command has a profound influence on the time course of the saccadic trajectory. It extends its effective dominant time constant to be greater than the plant, which is only 150 ms. That is, when the roll component is initiated during the saccade it will affect all direction cosines that then interact with each other as the eye moves through its trajectory.

In support of this idea we have simulated an experiment where saccades are made by humans looking around the corners of a square (Collewijn et al. 1988; Ferman et al. 1987). We have transformed our axis angle representation into Fick coordinates for this simulation (Figs. 2*A* and 11) so that it can be compared with the data that were recorded in Fick coordinates. The data show very slow "torsional angle" components during normal saccades in humans [Fig. 4 of Ferman et al. (1987)]. In many instances the torsional angle components would undershoot or overshoot their final value. The time constants were large and final eye orientation was not reached after 1 or 2 s (Ferman et al. 1987). The model predicts both overshoots and undershoots in the torsional angle components as well as the slow time course for the torsional angle component (Fig. 11). Despite the fact that the data were obtained in light and the simulations were performed in dark, the similarities of model predictions and the data were remarkable.

The conceptual approach used to develop the model is in

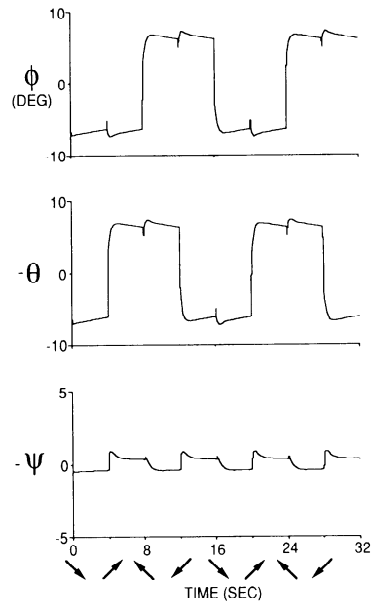

FIG. 11. Simulation of saccadic eye movements around the corners of a square in darkness. The angles ϕ, θ, and ψ are the Fick angles associated with horizontal, vertical, and torsional eye deviations, respectively (Fig. 2*A*). Simulated eye movements were transformed to this form to facilitate comparisons with data obtained by Ferman et al. (1987). Positive directions for the angles θ and ψ used by Ferman et al. (1987) are the negatives of the angles chosen in this study. Therefore the negative angles have been plotted. Arrows: directions from the primary position in which the eye is looking at each point on the square. For example, at time = 0, at the end of the saccade, the eye is looking down-right. At 4 s (end of saccade) the eye is looking up-right. At 8 s (end of saccade) it is looking up-left. At 12 s (end of saccade) it is looking down-left. This motion continues. Both horizontal (ϕ) and vertical ($-\theta$) eye movements are rapid. The decays between movement are due to the decay of the velocity-position integrator. The torsional component of eye movement, $-\psi$, has both overshoots and undershoots, as do the data of Ferman et al. (1987).

sharp contrast to that used for developing the "multiplicative quaternion model." The quaternion model was developed on the premise that a subtractive feedback implementation of the integrator cannot explain rotations in three dimensions (Crawford and Vilis 1991; Hepp and Henn 1987; Tweed and Vilis 1987, 1988). The key conceptual difference between the two modeling approaches is that although eye position is assumed to be the output of the integrator in the quaternion model (Tweed and Vilis 1987) it is not a signal generated by the velocity-position integrator in the present study. Rather, the model presented here uses the physiologically established fact that the CNS generates a torque signal that drives the eye muscles that orient the eyes. Thus the eyes will move to a position such that a state of equilibrium is reached between the applied torque and the restoring torque generated by the orbital tissues (Miller and Robinson 1984; Robinson 1975b). Because torque signals behave as vectors, they commute, and the order in which torque signals are applied to the eye will not affect the final orientation of the eye. Steady-state eye orientation will only be determined by the summation of the torques in any order. This blunts the criticism leveled against the classical velocity-position integrator that it does not take into account the noncommutative property of eye rotations in three dimensions (Hepp and Henn 1987; Tweed and Vilis 1987). The point is that it does not have to.

The quaternion model also does not predict the pulse-step or step-ramp characteristics of the motoneurons and how they would interact with the plant (Fuchs and Luschei 1970; Henn and Cohen 1973; Keller and Robinson 1972; Robinson 1970). It does not address the fact that there are time constants of decay associated with holding positions of fixation. More importantly, the quaternion model is not consistent with the fact that the motoneurons generate a signal to the eye muscles that generate torque and that eye orientation is not coded directly in their activity.

The prediction of our model regarding how Listing's law is implemented also stands in marked contrast to that predicted by the quaternion model (Haslwanter et al. 1991; Haustein 1989; Hepp 1990; Hepp and Henn 1987; Straumann et al. 1991; Tweed and Vilis 1987, 1988). Listing's law simply states that the eye will move only into positions of fixation that can be described by a rotation, from a primary orientation, about an axis in a head fixed plane known as Listing's plane (Haustein 1989; von Helmholtz 1962). To satisfy Listing's law, the quaternion model constrains the quaternion vector to lie in Listing's plane (Tweed and Vilis 1988). Because the quaternion model assumes that eye orientation i.e., the eye position quaternion, is encoded in the velocity-position integrator, it necessitates postulating a Listing's law operator as well as quaternion operations in the CNS to implement Listing's law (Tweed and Vilis 1990b). This organizational complexity of the system is unwarranted.

Central activity upstream of the immediate premotor site associated with saccadic eye movements also is not supported by the quaternion model. Robinson and Zee (1981) had suggested that Listing's law was implemented downstream of the superior colliculus at the level of the burst cells, whereas Tweed and Vilis (1990b), on the basis of their quaternion model, concluded that Listing's law was implemented upstream of the superior colliculus. Work performed on stimulating the superior colliculus (Van Opstal et al. 1991) yielded saccadic trajectories that were in the pitch-yaw plane with no torsional component. The conclusion from this study was that Listing's law was implemented downstream of the superior colliculus. In the model presented here, Listing's law is generated naturally if the pulses driving the velocity-position integrator have only pitch and yaw components and no roll components. Thus Listing's law is a general property of the vector nature of signals in the CNS and how they activate the velocity-position integrator. It is not linked to any specific site in the CNS. As long as the signals are confined to Listing's plane, i.e., the pitch-yaw plane in our model, Listing's law will be satisfied.

An interesting prediction of our model is that although Listing's law is satisfied during centripetal and centrifugal saccadic trajectories, it is only approximately satisfied during saccadic trajectories from secondary to tertiary positions. This prediction is in contrast to the predictions of the quaternion model, which, lacking dynamic components, demands that Listing's law be satisfied during the saccadic trajectory (Tweed and Vilis 1990a). The data that show the "plane of confinement" during saccadic eye movements (Haslwanter et al. 1992; Tweed and Vilis 1988, 1990a) do not support the contention that Listing's law is satisfied during saccades. For a wide range of saccades, the plane

associated with saccadic movements is "thick," having an SD from Listing's plane of $\leq 2°$. The plane is considerably thicker during saccades (Tweed and Vilis 1990a).

In our model simulations (Figs. 4 and 5) the roll component during a saccade from a secondary to a tertiary position has a direction cosine that transiently reaches a maximum of ~ 0.076. This corresponds to a maximum saccade axis tilt out of Listing's plane of $<5°$. The average tilt out of Listing's plane is much less. This is well within the confines of reported data on the accuracy of Listing's law. The deviations from Listing's law for pursuit in Figs. 9 and 10 are much smaller, being $<1°$. Thus our model not only predicts the closeness of saccadic and smooth pursuit trajectories to Listing's plane but also predicts the deviations, which the quaternion model does not.

The model presented here has a global significance regarding Listing's law. It predicts that any eye movement command signals that are encoded only in Listing's plane, i.e., the pitch-yaw plane in head coordinates, and are directed through the velocity-position integrator would obey Listing's law in the steady state. Thus slow phase eye movements made during pursuit should theoretically obey Listing's law if the driving signals are in the pitch-yaw plane. Confining signals to this plane would make sense as far as the CNS is concerned, because during pursuit there would be no need to issue torsional or roll command signals to drive the eyes. This prediction of the model is consistent with findings that smooth pursuit eye movements approximately obey Listing's law in the monkey (Haslwanter et al. 1991). In addition, Listing's law for head and arm movements (Straumann et al. 1991) could probably be modeled by extending the ideas presented in this study.

The model presented is limited in that the nonlinear length-tension relationship of muscles was not considered. In addition, the torque-orientation relationship may have some associated nonlinearities that were neglected. Also, the different gains in the transmission of signals associated with pitch, roll, and yaw eye movements were not incorporated into the model structure. In addition the model has not dealt with how pulses and steps that input and activate the velocity-position integrator are generated. Despite these shortcomings the model has a physiologically correct structure and demonstrates the following:

1) To rotate the eyes in three dimensions, the CNS uses a vector and not an orientation or quaternion code to generate saccades and smooth pursuit eye movements.

2) Velocity-position integration is simply a three-dimensional dynamical system extension of the one-dimensional model. Its output is a vector that drives motoneurons that generate torque in the eye muscles.

3) The nonvector orientation properties of eye movements arise from the torque-orientation relationship of the eye globe and its surrounding tissues and not in the velocity-position integrator.

Appendix A

To find $d\Phi/dt$ and $d\hat{\mathrm{n}}/dt$ as functions of orientation and eye velocity in the head, various expressions for the rate of change of R, dR/dt, are needed. The purpose of this appendix is to derive various expressions for $d\mathrm{R}/dt$ to be used in the body of the paper.

The change in $\hat{\mathrm{n}}$ with respect to time, $d\hat{\mathrm{n}}/dt$, due to the angular velocity of the rotation, ω, can be considered a transformation of a head fixed vector associated with the primary position, $\mathbf{r}(0)$, of the eye, by a time-varying rotation matrix, $R(t)$. The matrix $R(0)$ is the identity matrix and represents the primary orientation at $t = 0$. Therefore at any time, t, the vector $\mathbf{r}_0$, is transformed by the orientation matrix, $R(t)$ to $r(t)$ and is given by

$$\mathbf{r}(t) = R(t)\mathbf{r}_0 \tag{A1}$$

By differentiating *Eq.* A*1* we obtain

$$\frac{d\mathbf{r}(t)}{dt} = \frac{dR(t)}{dt}\mathbf{r}_0 \tag{A2}$$

Because the rate of change of $\mathbf{r}(t)$ is due to the angular velocity relative to the head, ω, an equivalent formula for the derivative of $\mathbf{r}$ can be given by (Goldstein 1980)

$$\frac{d\mathbf{r}(t)}{dt} = \omega \wedge r(t) \tag{A3}$$

where $\wedge$ represents the vector cross-product between two vectors. *Equation* A*3* can be expressed in matrix form as follows

$$\frac{d\mathbf{r}(t)}{dt} = \Omega\mathbf{r}(t) \tag{A4}$$

where

$$\Omega = \begin{pmatrix} 0 & -\omega_3 & \omega_2 \\ \omega_3 & 0 & -\omega_1 \\ -\omega_2 & \omega_1 & 0 \end{pmatrix} \tag{A5}$$

and

$$\omega = \begin{pmatrix} \omega_1 \\ \omega_2 \\ \omega_3 \end{pmatrix} \tag{A6}$$

Combining *Eq.* A*1* and A*4* we obtain

$$\frac{d\mathbf{r}(t)}{dt} = \Omega R\mathbf{r}_0 \tag{A7}$$

Comparing *Eq.* A*2* and A*7*, the rate of change of the rotation matrix can be given as

$$\frac{dR}{dt} = \Omega R \tag{A8}$$

By comparing *Eq.* A*3* and A*4* we obtain

$$\Omega\mathbf{r}(t) = \omega \wedge \mathbf{r}(t) \tag{A9}$$

Equation A*9* holds for any vector $\mathbf{r}(t)$. In addition, at any time, t, the orientation matrix, R, can be represented by three unit vectors that form its columns. The matrix, R, is given by

$$R(t) = [\mathbf{u}_1(t), \mathbf{u}_2(t), \mathbf{u}_3(t)] \tag{A10}$$

Therefore from *Eq.* A*8*, A*9*, and A*10* the rate of change of R can be given as

$$\frac{dR}{dt} = \Omega R(t) = [\omega \wedge \mathbf{u}_1(t), \omega \wedge \mathbf{u}_2(t), \omega \wedge \mathbf{u}_3(t)] \tag{A11}$$

Equation A*11* is a representation of how the orientation matrix, R, is affected over time as a result of the velocity vector ω.

Appendix B

In this appendix we derive an estimate of the pulse step ratio that is necessary to match the plant dynamics during a saccade. Assume that for a centrifugal saccade the plant can be approximated by a first-order system (Robinson 1973) given by

$$\frac{d\theta}{dt} = -\frac{1}{\tau}\theta + gm_{\mathrm{n}} \tag{B1}$$

where θ is the eye position, τ is its dominant time constant, g is the coupling of motoneurons to the plant, and m_{n} is the motoneuron input. If m_{n} is a pulse of amplitude A and duration d, then at the end of the pulse the eye will have reached a position

$$\theta_{\text{pulse}} = g\tau A(1 - e^{-d/\tau}) \quad \text{(B2)}$$

If m_n is a step input of amplitude S, the eye should eventually reach a steady-state condition for *Eq.* B*1*, which is given by

$$\theta_{\text{step}} = g\tau S \quad \text{(B3)}$$

For the pulse step to be matched so that the eye reaches a position and is held there, the position reached from the pulse input must be equal to the position reached from the step input after a long time. Therefore

$$\theta_{\text{pulse}} = \theta_{\text{step}} \quad \text{(B4)}$$

or

$$g\tau A(1 - e^{-d/\tau}) = g\tau S \quad \text{(B5)}$$

Therefore

$$\frac{A}{S} = = \frac{1}{1 - e^{-d/\tau}} \quad \text{(B6)}$$

For a saccade duration $d = 0.05$ s and a plant time constant of $\tau = 0.15$ s, the pulse step ratio is 3.5.

This work was supported by National Institute of Health Grants EY-04148, NIGMS MRC 5T34 08078, and PSC-CUNY Award 668285.
Address reprint requests to T. Raphan.

Received 23 December 1992; accepted in final form 29 September 1993.

REFERENCES

BECKER, W. AND KLEIN, H. Accuracy of saccadic eye movements and maintenance of eccentric eye positions in the dark. *Vision Res.* 13: 1021–1034, 1973.

COHEN, B. AND HENN, V. The origin of quick phases of nystagmus in the horizontal plane. *Bibl. Ophthalmol.* 82: 36–55, 1972a.

COHEN, B. AND HENN, V. Unit activity in the pontine reticular formation associated with eye movements. *Brain Res.* 46: 403–410, 1972b.

COHEN, B. AND KOMATSUZAKI, A. Eye movements induced by stimulation of the pontine reticular formation: evidence for integration in oculomotor pathways. *Exp. Neurol.* 36: 101–117, 1972.

COLLEWIJN, H., FERMAN, L., AND VAN DEN BERG, A. V. The behavior of human gaze in three dimensions. In: *Representation of Three-Dimensional Space in the Vestibular, Oculomotor, and Visual Systems,* edited by B. Cohen and V. Henn. New York: NY Acad. Sci., 1988, p. 105–127.

COLLINS, C. C. Orbital Mechanics. In: *The Control of Eye Movements,* edited by P. Bach-y-Rita, C. C. Collins, and J. E. Hyde. New York: Academic, 1971, p. 283–325.

COLLINS, C. C., SCOTT, A. B., AND O'MEARA, D. Elements of the peripheral oculomotor apparatus. *Am. J. Optom.* 46: 510–515, 1969.

COOK, G. AND STARK, L. Derivation of a model for the human eye-positioning mechanism. *Bull. Math. Biophys.* 29: 153–174, 1967.

CRAWFORD, J. D. AND VILIS, T. Axes of eye rotation and Listing's law during rotations of the head. *J. Neurophysiol.* 65: 407–423, 1991.

FERMAN, L., COLLEWIJN, H., AND VAN DEN BERG, A. V. A direct test of Listing's Law. II. Human ocular torsion measured under dynamic conditions. *Vision Res.* 27: 939–951, 1987.

FUCHS, A. F. AND LUSCHEI, E. S. Firing patterns of abducens neurons of alert monkeys in relationship to horizontal eye movement. *J. Neurophysiol.* 23: 382–392, 1970.

FUCHS, A. F. AND LUSCHEI, E. S. The activity of single trochlear nerve fibers during eye movements in the alert monkey. *Exp. Brain Res.* 13: 78–89, 1971.

GOLDSTEIN, H. *Classical Mechanics.* Reading, MA.: Addison-Wesley, 1980.

HASLWANTER, T., STRAUMANN, D., HEPP, K., HESS, B. J. M., AND HENN, V. Smooth pursuit eye movements obey Listing's law in the monkey. *Exp. Brain Res.* 87: 470–472, 1991.

HASLWANTER, T., STRAUMANN, D., HESS, B. J. M., AND HENN, V. Static roll and pitch in the monkey: shift and rotation in Listing's plane. *Vision Res.* 32: 1341–1348, 1992.

HAUSTEIN, W. Consideration on Listing's law and the primary position by means of a matrix description of eye position control. *Biol. Cybern.* 60: 411–420, 1989.

VON HELMHOLTZ, H. *Handbuch der Physiologischen Optik.* English translation: *Treatise on Physiological Optics.* New York: Dover, 1962.

HENN, V. AND COHEN, B. Quantitative analysis of activity in eye muscle motoneurons during saccadic eye movements and positions of fixation. *J. Neurophysiol.* 36: 115–126, 1973.

HENN, V. AND COHEN, B. Coding of information about rapid eye movements in the pontine reticular formation of alert monkeys. *Brain Res.* 108: 307–325, 1976.

HENN, V., STRAUMANN, D., HESS, B. J. M., HASLWANTER, T., AND KAWACHI, N. Three dimensional transformations from vestibular and visual input to oculomotor output. *Ann. NY Acad. Sci.* 656: 166–180, 1992.

HEPP, K. On Listing's Law. *Commun. Math. Phys.* 132: 285–292, 1990.

HEPP, K. AND HENN, V. Spatio-temporal recording of rapid eye movement signals in the monkey paramedian pontine reticular formation (PPRF). *Exp. Brain Res.* 52: 105–120, 1983.

HEPP, K. AND HENN, V. Nonabelian neurodynamics. In: *Physics in Living Matter, Lecture Notes in Physics,* edited by D. Baeriswyl, M. Droz, A. Malaspinas, and P. Martinolo. Heidelberg, Germany: Springer-Verlag, 1987, p. 163–177.

HEPP, K., HENN, V., VILIS, T., AND COHEN, B. Brainstem regions related to saccade generation. In: *The Neurobiology of Saccadic Eye Movements,* edited by R. Wurtz and M. Goldberg. Amsterdam: Elsevier, 1989, p. 105–211.

HEPP, K., VILIS, T., AND HENN, V. On the generation of rapid eye movements in three dimensions. *Ann. NY Acad. Sci.* 545: 140–153, 1988.

KELLER, E. Participation of medial pontine reticular formation in eye movement generation in monkey. *J. Neurophysiol.* 37: 316–332, 1974.

KELLER, E. L. AND ROBINSON, D. A. Absence of the stretch reflex in extraocular muscles of the monkey. *J. Neurophysiol.* 34: 908–919, 1971.

KELLER, E. L. AND ROBINSON, D. A. Abducens unit behavior in the monkey during vergence movements. *Vision Res.* 12: 369–382, 1972.

LEVIN, A. AND WYMAN, J. The viscous elastic properties of muscle. *Proc. R. Soc. Lond. B Biol. Sci.* 150: 218–243, 1927.

LUSCHEI, E. S. AND FUCHS, A. F. Activity of brain stem neurons during eye movements of alert monkeys. *J. Neurophysiol.* 35: 445–461, 1972.

MILLER, J. M. AND ROBINSON, D. A. A model of the mechanics of binocular alignment. *Comp. Biomed. Res.* 17: 436–470, 1984.

NAKAYAMA, K. Coordination of extraocular muscles. In: *Basic Mechanisms of Ocular Motility and Their Clinical Implications,* edited by G. Lennerstrand and P. Bach-Y-Rita. New York: Pergamon, 1975, p. 193–207.

NAKAYAMA, K. A new method of determining the primary position of the eye using Listing's law. *Am. J. Optom. Physiol. Opt.* 55: 331–336, 1978.

NAKAYAMA, K. AND BALLIET, R. Listing's Law, eye position sense, and perception of the vertical. *Vision Res.* 17: 453–457, 1977.

OPTICAN, L. M. AND MILES, F. A. Visually induced adaptive changes in primate saccadic oculomotor control signals. *J. Neurophysiol.* 54: 940–958, 1985.

OPTICAN, L. M. AND ROBINSON, D. A. Cerebellar-dependent adaptive control of primate saccadic system. *J. Neurophysiol.* 44: 1058–1076, 1980.

PIO, R. L. Euler angle transformations. *IEEE Trans. Autom. Control.* 11: 707–712, 1966.

RAPHAN, T. AND COHEN, B. Brainstem mechanisms for rapid and slow eye movements. *Annu. Rev. Physiol.* 40: 527–552, 1978.

ROBINSON, D. A. The mechanics of human saccadic eye movement. *J. Physiol Lond.* 174: 245–264, 1964.

ROBINSON, D. A. The mechanics of smooth pursuit eye movement. *J. Physiol. Lond.* 180: 569–591, 1965.

ROBINSON, D. A. Oculomotor unit behavior in the monkey. *J. Neurophysiol.* 33: 393–404, 1970.

ROBINSON, D. A. Models of the saccadic eye movement control system. *Kybernetic* 14: 71–83, 1973.

ROBINSON, D. A. Cerebellectomy and vestibulo-ocular reflex arc. *Brain Res.* 71: 215–224, 1974.

ROBINSON, D. A. Oculomotor control signals. In: *Basic Mechanisms of Ocular Motility and Their Clinical Implications,* edited by G. Lennerstrand and P. Bach-Y-Rita. Oxford: Pergamon, 1975a, vol. 24, p. 337–374.

ROBINSON, D. A. A quantitative analysis of extraocular muscle cooperation and squint. *Invest. Ophthalm.* 14: 801–825, 1975b.

ROBINSON, D. A. Control of eye movements. In: *Handbook of Physiology. The Nervous System. Motor Control.* Washington, DC: Am. Physiol. Soc., 1981, sect. 1, vol. II, p. 1275–1320.

ROBINSON, D. A., O'MEARA, D. M., SCOTT, A. B., AND COLLINS, C. C. The mechanical components of human eye movements. *J. Appl. Physiol.* 26: 548–553, 1969.

ROBINSON, D. A. AND ZEE, D. Theoretical considerations in the function and circuitry of various rapid eye movements. In: *Progress in Oculomotor Research, Developments in Neuroscience,* edited by A. Fuchs and W. Becker. Amsterdam: Elsevier/North-Holland, 1981, p. 3–12.

SKAVENSKI, A. AND ROBINSON, D. A. Role of abducens motoneurons in the vestibulo-ocular reflex. *J. Neurophysiol.* 36: 724–738, 1973.

STRAUMANN, D., HASLWANTER, T., HEPP-REYMOND, M.-C., AND HEPP, K. Listing's law for eye, head and arm movements and their synergistic control. *Exp. Brain Res.* 86: 209–215, 1991.

TWEED, D. AND VILIS, T. Implications of rotational kinematics for the oculomotor system in three dimensions. *J. Neurophysiol.* 58: 832–849, 1987.

TWEED, D. AND VILIS, T. Rotation axes of saccades. *Ann. NY Acad. Sci.* 545: 128–139, 1988.

TWEED, D. AND VILIS, T. Geometric relations of eye position and velocity vectors during saccades. *Vision Res.* 30: 111–127, 1990a.

TWEED, D. AND VILIS, T. The superior colliculus and spatiotemporal translation in the saccadic system. *Neural Networks* 3: 75–86, 1990b.

VAN GISBERGEN, J. A. M., ROBINSON, D. A., AND GIELEN, S. A quantitative analysis of saccadic eye movements by burst neurons. *J. Neurophysio.* 45: 417–442, 1981.

VAN OPSTAL, A. J., HEPP, K., HESS, B., STRAUMANN, D., AND HENN, V. Two-, rather than three-dimensional representation of saccades in monkey superior colliculus. *Science Wash. DC* 252: 1313–1315, 1991.